



Published in final edited form as:

Arterioscler Thromb Vasc Biol. 2013 January ; 33(1): 114–120. doi:10.1161/ATVBAHA.112.300278.

Cadherin-11 regulates cell-cell tension necessary for calcific nodule formation by valvular myofibroblasts

Joshua D. Hutcheson^{1,*}, Joseph Chen^{1,*}, M.K. Sewell-Loftin¹, Larisa M. Ryzhova¹, Charles I. Fisher¹, Yan Ru Su², and W. David Merryman^{1,+}

¹Department of Biomedical Engineering, Vanderbilt University, Nashville, TN

²Department of Medicine, Division of Cardiovascular Medicine, Vanderbilt University, Nashville, TN

Abstract

Objective—Dystrophic calcific nodule formation *in vitro* involves differentiation of aortic valve interstitial cells (AVICs) into a myofibroblast phenotype. Interestingly, inhibition of the kinase MEK1/2 prevents calcific nodule formation despite leading to myofibroblast activation of AVICs, indicating the presence of an additional mechanotransductive component required for calcific nodule morphogenesis. In this study, we assess the role of TGF- β 1-induced cadherin-11 expression in calcific nodule formation.

Methods and Results—As shown previously, porcine AVICs treated with TGF- β 1 prior to cyclic strain exhibit increased myofibroblast activation and significant calcific nodule formation. In addition to an increase in contractile myofibroblast markers, TGF- β 1 treated AVICs exhibit significantly increased expression of cadherin-11. This expression is inhibited by the addition of U0126, a specific MEK1/2 inhibitor. The role of increased cadherin-11 is revealed through a wound assay, which demonstrates increased intercellular tension in TGF- β 1 treated AVICs possessing cadherin-11. Furthermore, when siRNA is used to knockdown cadherin-11, calcific nodule formation is abrogated, indicating that robust cell-cell connections are necessary in generating tension for calcific nodule morphogenesis. Finally, we demonstrate enrichment of cadherin-11 in human calcified leaflets.

Conclusions—These results indicate the necessity of cadherin-11 for dystrophic calcific nodule formation, which proceeds through an Erk1/2 dependent pathway.

INTRODUCTION

The differentiation of quiescent fibroblasts to activated myofibroblasts represents a normal physiological response to injury *in vivo*; however, persistence of the myofibroblast phenotype contributes to a spectrum of fibrotic disease.^{1–4} Activated myofibroblasts are characterized by increased contractility due to smooth muscle alpha-actin (α SMA), and in normal physiology, these cells remodel the extracellular matrix (ECM) by secreting

*For correspondence: Department of Biomedical Engineering, Vanderbilt University, 2213 Garland Ave., 9445 MRB IV, Nashville, TN 37232-0493, P: 615.322.7219, F: 615.343.6541, david.merryman@vanderbilt.edu.

+co-first authors

Publisher's Disclaimer: This is a PDF file of an unedited manuscript that has been accepted for publication. As a service to our customers we are providing this early version of the manuscript. The manuscript will undergo copyediting, typesetting, and review of the resulting proof before it is published in its final citable form. Please note that during the production process errors may be discovered which could affect the content, and all legal disclaimers that apply to the journal pertain.

Disclosures

None.

proteases for matrix breakdown and *de novo* ECM components such as collagen¹⁻² Failure of the myofibroblasts to apoptose or return to quiescence in pathological cases causes impairment of organ systems due to elevated contractions and accumulation of ECM components. One disease in which the myofibroblast is thought to play a crucial role is calcific aortic valve disease (CAVD).⁵⁻¹⁰

Increased α SMA expression in aortic valve interstitial cells (AVICs), the resident fibroblast population in the aortic valve, has been observed in excised fibrotic leaflets.¹¹ Increased expression of the profibrotic cytokine transforming growth factor β 1 (TGF- β 1) has also been observed in these leaflets, and accordingly, TGF- β 1 has been shown to lead to myofibroblast activation of AVICs *in vitro*¹¹⁻¹³ Additionally, in *ex vivo* models of CAVD, TGF- β 1 works synergistically with mechanical strain to lead to collagen accumulation, characteristic of early CAVD, and formation of bone-like calcific nodules, an endpoint of CAVD.¹⁴⁻¹⁵ Two distinct calcific nodule morphologies have been observed: dystrophic calcification driven by myofibroblastic phenotypes¹⁶⁻¹⁸ and ossification driven by osteogenic phenotypes.¹⁹⁻²⁰ In diseased explants, dystrophic calcification and ossification has been observed in 83% and 13% of explanted diseased valves, respectively.²¹

In vitro, dystrophic nodule formation involves myofibroblast differentiation of AVICs. Upregulation of α SMA during myofibroblast differentiation by TGF- β 1 leads to an increase in mechanical tension between AVICs and subsequent aggregation into nodules, which calcify through apoptotic processes.^{13, 22} When α SMA expression is suppressed, calcific nodules are unable to develop thereby revealing the essential role of acquired contractility within AVICs in calcific nodule formation.¹⁶ Confoundingly, preventing phosphorylation of Erk1/2 with a MEK1/2 inhibitor leads to increased α SMA expression²³ yet prevents calcific nodule formation,²⁴ suggesting the requirement of another essential component of nodule formation that has yet to be revealed.

Along with increased α SMA expression, myofibroblast differentiation has been associated with changes in cadherin expression. Specifically, in lung fibroblasts, TGF- β 1-induced myofibroblast differentiation leads to an increase of cadherin-11 (aka OB-cadherin) and a decrease of N-cadherin.²⁵ Increased cadherin-11 expression has been implicated in various pathologies including pulmonary fibrosis and arthritis.²⁶⁻²⁷ Functionally, the transition to cadherin-11 yields stronger intercellular connections that improve force development in myofibroblast populations. Recent works have shown that elevated intercellular tension along with increased contractility drive calcific nodule formation of AVICs *in vitro*.¹⁶⁻¹⁷ Therefore, we hypothesize that TGF- β 1 induced cadherin-11 expression through an Erk1/2 dependent pathway is essential for robust cell-cell connections necessary for generating intercellular tension required for calcific nodule formation.

To test this hypothesis, we quantified the expression and contributions of cadherin-11 in calcific nodule formation of AVICs. Here, we show that TGF- β 1 induced myofibroblast differentiation of AVICs leads to upregulation of α SMA and cadherin-11 expression in an Erk1/2 dependent fashion, corresponding to increased functional contractility and cell-cell connection strength, respectively. Subsequent knockdown of cadherin-11 inhibits the ability of AVICs to generate calcific nodules similar to knockdown of α SMA,¹⁶ demonstrating that both proteins are necessary for dystrophic calcific nodule morphogenesis.

METHODS

AVIC isolation and culture

Porcine aortic valve leaflets were excised from sacrificed animals within 10 minutes of slaughter at a local abattoir. Leaflets were stored in phosphate buffered saline (PBS) at 4°C

to ensure survival. Within 3 hours (h) of sacrifice, AVICs were isolated as previously described.²⁸ Briefly, after the removal of the endothelium, the leaflet was minced into 1 mm² pieces and digested in a 1 mg/ml collagenase solution (Worthington Biochemical Corp., Lakewood, NJ) for 1 h at 37° C and 5% CO₂. The collagenase solution with the remaining tissue was passed through a cell strainer to collect a cell solution which was centrifuged at 1500 RPM for 5 min to obtain the cell pellet. The pellet was resuspended in Dulbecco's Modified Eagle Medium (DMEM) supplemented with 10% fetal bovine serum (FBS) (Atlanta Biological; Lawrenceville, GA), and 1% Antibiotic-Antimycotic (Gibco; Grand Island, NY). The cells were seeded on tissue culture dishes and incubated at 37° C and 5% CO₂ with media changes every three days. AVICs were cryopreserved after the second passage and all experiments in this study were performed using AVICs between passages 3–6.

Calcific Nodule Treatments and Analyses

AVICs were seeded onto BioFlex Proectin culture plates (Flexcell International Corporation) at a density of 60,000 cells/cm² in 3 ml of media. After reaching confluence (~48 h), AVICs were treated with 1 ng/mL TGF-β1, 10 μM U0126, a MEK1/2 inhibitor that prevents Erk1/2 phosphorylation, or U0126 + TGF-β1 for 24 h, after which they were subjected to 15% cyclic equibiaxial strain via the Flexcell-4000 tension system (Flexcell International Corporation) at a frequency of 0.75 Hz for 24 h. The specific sequence of TGF-β1 for 24 h followed by 15% cyclic strain results in the formation of dystrophic calcific nodules.¹⁷

To quantify nodule counts following treatments, AVICs were rinsed twice with PBS and fixed in 3.7% neutral buffered formaldehyde for 15 min. AVICs were rinsed with PBS and, unless immediately stained, stored at 4°C for up to several days. Each 35 mm well was rinsed with deionized water (dH₂O) and stained with 1 ml of 14 mM Alizarin red S (Sigma) (in dH₂O, pH 4.1, where undissolved particulates were removed with a 0.45μm filter) for 30 min with agitation to determine calcium deposition. After staining, the cells were washed 4 times with dH₂O to remove excess dye. Positively stained nodules were manually counted under the microscope.

To examine the morphology of the nodules formed following treatments, wells were rinsed with PBS and stained with Annexin V conjugated with Alexa fluor 488 (5% solution in Annexin binding buffer; Invitrogen) for 15 minutes to detect apoptotic cells. Propidium Iodide (0.4% solution in Annexin binding buffer; Invitrogen) was used as a counter-stain for necrotic cells. Images were taken with a Nikon TE300 inverted tissue culture fluorescence microscope.

Wound Assay

A wound assay to quantify the level of intercellular tension was performed as described previously.¹⁷ Briefly, AVICs were seeded on tissue culture polystyrene 6-well plates at 60,000 cells/cm² and allowed to adhere overnight. AVICs were treated with either 1 ng/ml TGF-β1, 10 μM U0126, or a combination of these treatments for 24 h. Prior to the introduction of a wound to the monolayer with a pipet tip, the extracellular growth media was washed away and replaced with DMEM media containing 1.8 mM Ca²⁺ or DMEM diluted with Ca²⁺ free PBS to give a final concentration of 0.45 mM Ca²⁺ 5 min prior to wounding in order to select for function of different cadherins. All cadherins require extracellular Ca²⁺ for function; however, cadherin-11 functions at lower Ca²⁺ concentrations than normal cadherins such as N-cadherin. Previous studies have identified 0.3 – 0.8 mM as a threshold concentration range in which cadherin-11 is functional but N-

cadherins display reduced functionality in this range.²⁹ Immediately after wounding, each well was imaged, and wound areas were calculated using ImageJ analysis software.

Protein and mRNA Assays

AVIC activation was quantified by assaying for α SMA protein expression using an indirect ELISA as described previously.^{17, 30} AVIC mRNA was isolated per manufacturer protocol using RNeasy isolation kit (Qiagen) and qPCR for α SMA (f: AACCGGGAGAAGATGACCCAGATT; r: ACCATCTCCAGAGTCCAGCACAAT) and cadherin-11 (f: CAAGTTAGTGACAGTATCCTGG; r: GTCTTTAGCCTTCACTCTCC) was performed on the HT7900 sequence detection system (Applied Biosystems, VUMC DNA Resource Core). β -actin was used as a housekeeping gene.

Immunofluorescence

AVICs were plated on fibronectin functionalized coverslips and treated with 1 ng/mL TGF- β 1, 10 μ M U0126, or U0126 + TGF- β 1 for 24 h. The cells were then fixed in 3.7% formaldehyde, permeabilized with 0.1% Triton X-100, and blocked with 1% bovine serum albumin for 1 h at room temperature. A primary antibody to cadherin-11 (2 μ g/ml, Santa Cruz) was added to the coverslips for 3 h at room temperature. After thorough washing in PBS, a fluorescently labeled secondary antibody (Alexa Fluor 488, Invitrogen) was added to the coverslip for 1 h. The coverslips were then washed and sealed with ProLong Gold antifade reagent (Invitrogen) overnight prior to imaging with a Nikon Eclipse E800 equipped with a Spot RT3 camera.

siRNA Knockdown

The necessity of cadherin-11 expression in intercellular tension and calcific nodule morphogenesis was assessed using siRNA knockdown. Cadherin-11 specific siRNA was designed using specialized algorithms, and 40 pM of each of three different siRNA duplexes (CCAAGTTAGTGACAGTAT, GGGATGGATTGTTGAA, CCTTATGACTCCATCCAAA, Sigma) were pooled and transfected into AVICs using Lipofectamine 2000 (Invitrogen) for 6 h. AVICs were then allowed to reach confluence (~72 h) prior to the addition of TGF- β 1 for calcific nodule assay or wounding assay, as described above. Live/Dead stain was conducted to assess cell viability following siRNA; Western blotting was used to confirm cadherin-11 knockdown efficiency at 96 h post-transfection, which was just prior to the application of strain or wounding.

Immunofluorescence, von Kossa staining, and mRNA analysis of human aortic valves

Human aortic valve leaflets were obtained from heart transplant recipients. Patients were enrolled in the Vanderbilt Heart and Vascular Institute Main Heart Registry, under an approved IRB protocol (#90828). Immediately after the heart was explanted, the aortic valve leaflets were dissected and flash frozen in the liquid nitrogen. A small piece of aortic valve was embedded in OCT and stored at -80°C . Calcified aortic valve leaflets were obtained from a 58 year old male patient with severe aortic valve stenosis and a 52 year old female with ischemic heart failure and notable fibrotic aortic valve leaflets, but no stenosis or visible calcific nodules. Because of the state and size of the tissue, we performed qPCR on the leaflet with severe aortic stenosis and immunofluorescence on the fibrotic leaflet. Non-calcified leaflets were obtained from unmatched organ donors, both were male, 51 and 47 years old, respectively, with no previous history of cardiovascular disease. For immunofluorescence, OCT embedded aortic valve leaflets were cut in 5–7 μ m sections, and incubated at room temperature with PBS. Tissue sections were stained for 4h at room temperature using a rabbit primary antibody to cadherin-11 (2.5 μ g/ml, Cell Signaling,

Danvers, MA), rinsed 3X in PBS with 0.01% Triton-X 100, incubated with an Alexa-Fluor 647-conjugated goat-anti-rabbit secondary antibody (6.6 $\mu\text{g}/\text{ml}$, Invitrogen, Grand Island, NY) and a primary antibody to αSMA directly conjugated with Cy3 (5 $\mu\text{g}/\text{ml}$, Sigma-Aldrich, St. Louis, MO), and finally washed 3X in PBS with 0.1% Triton-X 100. Excess moisture was carefully wicked away before samples were mounted in ProLong Gold AntiFade with DAPI (Invitrogen) and allowed to dry overnight at room temperature. All sections were imaged using the Nikon Eclipse 80i microscope. Adjacent sections were analyzed using a von Kossa calcium staining kit (PolySciences Inc., Warrington, PA). Total RNA was isolated using miRNeasy Mini kit (Qiagen) following manufacture instructions. qPCR for cadherin-11 (f:CAAGTTAGTGTACAGTATCCTCG; r:GATCTTTAGCTTTCACTCTTCT) and αSMA (f: ACAACAGCATCAGTAAGTGT; r:CATCGTATTCTGTTTGCTGA) as described above.

Statistical analyses

Data are reported as the mean of all replicates, and error is given as standard error of the mean ($n = 3$). Statistical significance between treatments was determined by one-way ANOVA, and pairwise differences were identified using post-hoc Holm-Sidak testing.

RESULTS

αSMA Expression is Not Sufficient for Calcific Nodule Formation in a Strain Environment

Consistent with previous results,²³ treating AVICs with either 1 ng/ml TGF- β 1 or 10 μM U0126 leads to a significant increase in αSMA mRNA and protein expression (Fig. 1A). A combination of these treatments also significantly increases αSMA expression compared to non-treated controls. As shown previously,¹⁷ AVICs treated with TGF- β 1 prior to the addition of strain form significantly more calcific nodules compared to non-treated, strained control AVICs (Fig. 1B), and calcific nodules were determined to be dystrophic with an apoptotic ring surrounding a necrotic core (Fig. 1B, **inset**). The addition of U0126 to the TGF- β 1 treatment prevents this increase in calcific nodule formation.

Erk1/2 Inhibition Does Not Affect Canonical TGF- β 1 Signaling

U0126 is a specific inhibitor to MEK1/2, the kinase directly upstream of the MAPK Erk1/2. Therefore, we assessed the effect of TGF- β 1 and U0126 on Erk1/2 phosphorylation in AVICs. Treating AVICs with TGF- β 1 for 1 h significantly increased Erk1/2 phosphorylation (Fig. 2A), and this phosphorylation is completely inhibited by the U0126 treatment. We next determined potential off target effects of U0126 treatment at other common TGF- β 1 signaling proteins. TGF- β 1 treatment for 1 h induces significant phosphorylation of its canonical transcription factor Smad3 (pSmad3) in a manner that is not inhibited by U0126 treatment (Fig. 2A). In addition to Smad3, we have previously shown that 1 h of TGF- β 1 treatment leads to phosphorylation of the MAPK p38 that is necessary for TGF- β 1-induced αSMA expression in AVICs.³⁰ Treating AVICs with U0126 does not inhibit TGF- β 1 p38 phosphorylation (Fig. 2A). Consistent with the pSmad3 results, treating AVICs with TGF- β 1 for 24 h leads to a significant increase in PAI-1 promoter luciferase activity that is not inhibited by U0126 treatment (Fig. 2B).

Erk1/2 Inhibition Suppresses TGF- β 1 Induced Expression of Cadherin-11

AVICs treated with TGF- β 1 for 24 h exhibit a significant increase in cadherin-11 mRNA that is inhibited by treating AVICs with U0126 (Fig. 3A). Immunofluorescence images also indicate changes in cadherin-11 expression and cellular localization following the TGF- β 1 and U0126 treatments (Fig. 3B). TGF- β 1 treated AVICs have visible cadherin-11 expression as indicated by FITC fluorescence between adjacent cells (with nuclei indicated

by DAPI staining). Expression of cadherin-11 was not observed in AVICs treated with U0126 or in non-treated controls.

Cadherin-11 is Required for Elevated Intercellular Tension and Calcific Nodules

Given that TGF- β 1 induces expression of cadherin-11 in a manner that is inhibited by U0126, we next determined if upregulation of this protein plays a role in increased intercellular tension that is believed to lead to the formation of dystrophic calcific nodules *in vitro*. When a wound is introduced to statically cultured AVICs in 1.8 mM Ca²⁺, a concentration that allows all cadherins to function, all treatment groups display increased intercellular tension as shown by larger wound areas compared to non-treated controls (Fig. 4A). However, when a wound is applied to AVICs in 0.45 mM Ca²⁺ media, a concentration that permits functionality of cadherin-11 but below the functional concentration for typical cadherins, only TGF- β 1 treated AVICs exhibit a significantly increased wound area, and this area is even greater than AVICs treated with TGF- β 1 and wounded in physiologic Ca²⁺ media. Because the low Ca²⁺ condition is not specific to cadherin-11, we knocked down cadherin-11 at physiologic calcium conditions (1.8 mM) with siRNA and found that this significantly reduced wound area after TGF- β 1 treatment (Fig. 4B).

To determine if cadherin-11 expression is necessary for calcific nodule formation, we used siRNA to knockdown cadherin-11 in AVICs. AVICs treated with lipofectamine transfection reagent alone or in combination with a non-specific scramble siRNA construct generated robust calcific nodules following TGF- β 1 treatment for 24 h and mechanical strain for an additional 24 h; however, AVICs transfected with siRNA specific to cadherin-11 did not develop calcific nodules (Fig. 4C). Introduction of siRNA for cadherin-11 did not affect viability (Fig. SI); no significant differences were observed for AVIC morphology and growth.

Expression of Cadherin-11 is Elevated in Calcified Human Aortic Valves

We evaluated non-calcified and calcified aortic valve leaflets from human explants with Von Kossa staining for calcification and immunohistochemistry for cadherin-11 and α SMA expression. Von Kossa staining revealed dramatic differences in the diseased valve with a significant accumulation of stain over the majority of the tissue (Fig. 5A,B). Immunostaining of the leaflets revealed the presence of cadherin-11 in non-calcified valves but very little α SMA expression. Cadherin-11 was prevalent near the periphery of the tissue confirming previous findings of its presence in the endothelium³¹ (Fig. 5A). However, in the calcified valve, cadherin-11 was highly expressed and co-localized with α SMA (Fig. 5B, **panels a and b**). Furthermore, in contrast to the peripheral staining observed in the non-calcified leaflet, cadherin-11 was detected throughout the interstitium of the leaflet but was not co-localized with α SMA in regions of diffuse calcium staining with von Kossa (Fig. 5B, **panel c**). qPCR revealed a 50-fold increase in cadherin-11 and ~10-fold increase in α SMA mRNA in the calcified leaflet when compared to non-calcified leaflets.

DISCUSSION

Dystrophic calcification in CAVD has been associated with the pathological differentiation of AVICs to myofibroblasts, which is characterized by increased α SMA expression. Treating AVICs with U0126, however, indicates that the presence of α SMA is not sufficient to drive dystrophic calcification, leading to the hypothesis that there exist other relevant mechanisms that have not been elucidated. Here, we present evidence that TGF- β 1 treatment of AVICs leads to expression of the atypical cadherin, cadherin-11, and expression of this intercellular adhesion protein is necessary for the development of dystrophic calcific nodules *in vitro*.

Previous *in vitro* studies on dystrophic calcific nodule formation revealed the importance of α SMA as a mediator of the process. TGF- β 1 treatment of AVICs led to increased expression of α SMA, which reinforces stress fibers and produces a more contractile cell. Benton et al. showed this increased contractility leads to contraction events that result in cell aggregates that develop into calcific nodules through an apoptosis driven pathway.¹⁶ Recently, we found that mechanical strain exacerbated the formation of these aggregates by introducing a force imbalance on the monolayer whereby increased intercellular tension is overcome by the addition of externally applied strain.¹⁷ This led us to theorize that TGF- β 1 induced myofibroblast populations possessed higher intercellular tension than quiescent fibroblasts, thus making them more sensitive to mechanical strain and subsequent nodule formation.

Interestingly, distinct differences in cadherin expression have been observed in fibroblast and myofibroblastic populations with fibroblasts expressing N-cadherin and myofibroblasts expressing cadherin-11.²⁵ Cadherin-11 junctions withstand two-fold higher forces when compared to connections formed with N-cadherin.³² Furthermore, upon application of forces, cadherin-11 expressing cells will continue to hold on and eventually rip at the plasma membrane while N-cadherin expressing cells release from each other.²⁵ These stronger intercellular contacts are organized by and work synergistically with increased α SMA expression leading to the accumulation of tension within myofibroblast populations. To test the effect of cadherin-11 on elevated intercellular tension, we utilized a wound assay as described previously;¹⁷ however, in this study we varied the concentration of extracellular Ca^{2+} to select for function of different cadherins. All cadherins require the presence of extracellular Ca^{2+} in order to function, but atypical cadherins such as cadherin-11 have a higher Ca^{2+} affinity ($K_D \sim 0.2 \text{ mM}$) than normal cadherins.²⁹ Therefore, cadherin-11 functions at lower Ca^{2+} concentrations than normal cadherins such as N-cadherin ($K_D = 0.7\text{mM}$). This difference in cadherin Ca^{2+} affinity is reflected in the wound assay results. At physiologic Ca^{2+} concentration, all cadherins are functional. TGF- β 1 and U0126 treatments both lead to an increase in α SMA, thus an increase in AVIC contractility; therefore, these two treatment groups cause significant tension as the AVICs pull on each other in the monolayer, ultimately leading to large increases in wound area. When the extracellular Ca^{2+} is lowered such that only cadherin-11 is functional, intercellular tension does not build in the U0126 treated AVICs, and the wound area for this treatment group is not significantly different than non-treated controls. However, for TGF- β 1 treated AVICs in the low Ca^{2+} case, the presence of cadherin-11 in AVICs treated with TGF- β 1 alone allows intercellular tension to build in the monolayer, leading to a significant increase in wound area compared to non-treated control samples. Additionally, since typical surface-adhesion cadherins are weaker in the low Ca^{2+} case, the increased force imbalance leads to an even larger wound area for AVICs treated with TGF- β 1 compared to the physiologic Ca^{2+} case. Illustrating the importance of increased tension conferred by cadherin-11 expression in nodule formation, when siRNA is used to knockdown the expression of cadherin-11, intercellular tension is reduced and calcific nodules fail to form after TGF- β 1 treatment and mechanical strain. This indicates that robust cell-cell connectivity in conjunction with contraction events are both necessary for calcific nodule formation.

From this, we propose the following model of calcific nodule morphogenesis. Activated AVICs express two mechanotransductive proteins due to TGF- β 1: α SMA and cadherin-11. With the change in protein expression, there is a dramatic change in the physical interaction between the cells in the monolayer. Intercellular tension increases as the cells become tightly connected due to cadherin-11 and as the cells become contractile due to α SMA. Eventually, the increased tension throughout the monolayer generates an imbalance of forces possibly due to cadherin-11 expression differences within individual cells. The application of external forces, such as large tissue deformation during valve closure,

increases this tension imbalance leading to apoptosis of the weaker cell and creating aggregates as the initiating step of calcific nodule morphogenesis. Calcific nodules mature as cells near the periphery of the aggregate experience strain magnification due to the non-deformity of the nodule, leading to apoptosis and calcification, as we proposed recently.¹⁷

Expression of cadherin-11 by TGF- β 1 is blocked by pre-treating AVICs with U0126, an inhibitor to MEK1/2. MEK1/2 is a MAPK kinase that when activated leads to phosphorylation of the MAPK Erk1/2. TGF- β 1-induced phosphorylation of Erk1/2 has been observed in a wide-variety of cell types and has been shown to be necessary for numerous cellular responses^{33–35}. Activation of Erk1/2 has also been shown to suppress α SMA expression in mouse embryonic fibroblasts.³⁶ Consistently, U0126 treatment leads to a significant increase in α SMA expression in AVICs. Our previous results indicate that TGF- β 1-induced expression of α SMA in AVICs requires phosphorylation of a different non-canonical MAPK p38.³⁰ Therefore, it seems that these two non-canonical pathways may independently lead to expression of proteins that are characteristic of pathological differentiation of AVICs. In contrast, canonical TGF- β 1 signaling leads to increased expression of PAI-1, and we have hypothesized that upregulation of PAI-1 through activation of the canonical Smad2/3 pathway may be involved a negative feedback of TGF- β 1 signaling.³⁰ Therefore, the results of these studies suggest a divergence in TGF- β 1 signaling that leads to AVIC myofibroblastic differentiation through activation of non-canonical pathways (p38 and Erk1/2) that each lead to a different cellular outcome that may be very important in CAVD, while canonical Smad pathways may not be directly involved in pathological signaling for CAVD. Additionally, Erk1/2 phosphorylation has been shown to be required for mechanically-induced calcific mineralization by calcifying vascular cells,³⁷ suggesting that these pathways may be important in a variety of calcification processes. We believe that the results of this study suggest a therapeutic approach for CAVD by targeting either of these non-canonical pathways or direct inhibition of cadherin-11 function.

Finally, we do show here the presence of increased cadherin-11 in calcified human aortic valve leaflets, which is co-localization with α SMA. The drastic changes in cadherin-11 in the calcified leaflets (Fig. 5) is supported by a recent report of significant cadherin-11 mRNA upregulation in stenotic human leaflets versus non-stenotic leaflets.³⁸ Mechanistically, this seems reasonable as sclerosis often causes stenosis, both of which precede calcification. In order for the current work to realize a larger clinical impact, the *in vitro* mechanisms and AVIC outcomes identified in this study should be examined *in vivo*. However, *in vivo* research into the mechanisms of CAVD is currently limited by the lack of an animal model that accurately recapitulates human pathology. Nonetheless, we believe that identification of cadherin-11 may provide a useful tool for better understanding the pathogenesis of CAVD, and these results may have implications beyond solely elucidating mechanisms of calcific nodule formation. AVIC myofibroblast activation is believed to be one the earliest processes in CAVD; however, early valvular changes are difficult to detect in patients. Very few markers of this differentiation are known, and the most commonly used ones such as α SMA do not lend themselves to imaging techniques due to their cytosolic expression. Since cadherin-11 is a transmembrane protein, it allows for targeting via molecular imaging tracers and may provide a molecular fingerprint for the onset of CAVD.

Supplementary Material

Refer to Web version on PubMed Central for supplementary material.

Acknowledgments

The authors thank the Vanderbilt Heart and Vascular Institute Main Heart Registry for supplying the diseased leaflets and supporting the study. We also thank Tarek Absi, MD for supplying the non-calcified aortic valve leaflets.

Sources of Funding

This work was supported by the AHA (0835496N and 09GRNT2010125) and NIH (HL094707), all to WDM. JDH (10PRE4290020), JC (11PRE7990023), and MKSL (12PRE12070154) were supported by AHA Pre-doctoral Fellowships.

REFERENCES

1. Hinz B. Formation and function of the myofibroblast during tissue repair. *J Invest Dermatol.* 2007; 127:526–537. [PubMed: 17299435]
2. Tomasek JJ, Gabbiani G, Hinz B, Chaponnier C, Brown RA. Myofibroblasts and mechano-regulation of connective tissue remodelling. *Nat Rev Mol Cell Biol.* 2002; 3:349–363. [PubMed: 11988769]
3. Hinz B. The myofibroblast: Paradigm for a mechanically active cell. *J Biomech.* 2010; 43:146–155. [PubMed: 19800625]
4. Serini G, Gabbiani G. Mechanisms of myofibroblast activity and phenotypic modulation. *Exp Cell Res.* 1999; 250:273–283. [PubMed: 10413583]
5. Goldberg SH, Elmariah S, Miller MA, Fuster V. Insights into degenerative aortic valve disease. *J Am Coll Cardiol.* 2007; 50:1205–1213. [PubMed: 17888836]
6. Freeman RV, Otto CM. Spectrum of calcific aortic valve disease: Pathogenesis, disease progression, and treatment strategies. *Circulation.* 2005; 111:3316–3326. [PubMed: 15967862]
7. Helse S, Kupari M, Lindstedt KA, Kovanen PT. Aortic valve stenosis: An active atheroinflammatory process. *Curr Opin Lipidol.* 2007; 18:483–491. [PubMed: 17885417]
8. Mohler ER 3rd, Chawla MK, Chang AW, Vyavahare N, Levy RJ, Graham L, Gannon FH. Identification and characterization of calcifying valve cells from human and canine aortic valves. *J Heart Valve Dis.* 1999; 8:254–260. [PubMed: 10399657]
9. Rajamannan NM. Calcific aortic valve disease: Cellular origins of valve calcification. *Arterioscler Thromb Vasc Biol.* 2011; 31:2777–2778. [PubMed: 22096095]
10. Rajamannan NM, Evans FJ, Aikawa E, Grande-Allen KJ, Demer LL, Heistad DD, Simmons CA, Masters KS, Mathieu P, O'Brien KD, Schoen FJ, Towler DA, Yoganathan AP, Otto CM. Calcific aortic valve disease: Not simply a degenerative process: A review and agenda for research from the national heart and lung and blood institute aortic stenosis working group. Executive summary: Calcific aortic valve disease-2011 update. *Circulation.* 2011; 124:1783–1791. [PubMed: 22007101]
11. Chen JH, Chen WL, Sider KL, Yip CY, Simmons CA. Beta-catenin mediates mechanically regulated, transforming growth factor-beta1-induced myofibroblast differentiation of aortic valve interstitial cells. *Arterioscler Thromb Vasc Biol.* 2011; 31:590–597. [PubMed: 21127288]
12. Cushing MC, Liao JT, Anseth KS. Activation of valvular interstitial cells is mediated by transforming growth factor-beta1 interactions with matrix molecules. *Matrix Biol.* 2005; 24:428–437. [PubMed: 16055320]
13. Walker GA, Masters KS, Shah DN, Anseth KS, Leinwand LA. Valvular myofibroblast activation by transforming growth factor-beta: Implications for pathological extracellular matrix remodeling in heart valve disease. *Circ Res.* 2004; 95:253–260. [PubMed: 15217906]
14. Balachandran K, Sucusky P, Jo H, Yoganathan AP. Elevated cyclic stretch induces aortic valve calcification in a bone morphogenic protein-dependent manner. *Am J Pathol.* 177:49–57. [PubMed: 20489151]
15. Merryman WD, Lukoff HD, Long RA, Engelmayr GC Jr, Hopkins RA, Sacks MS. Synergistic effects of cyclic tension and transforming growth factor-beta1 on the aortic valve myofibroblast. *Cardiovasc Pathol.* 2007; 16:268–276. [PubMed: 17868877]

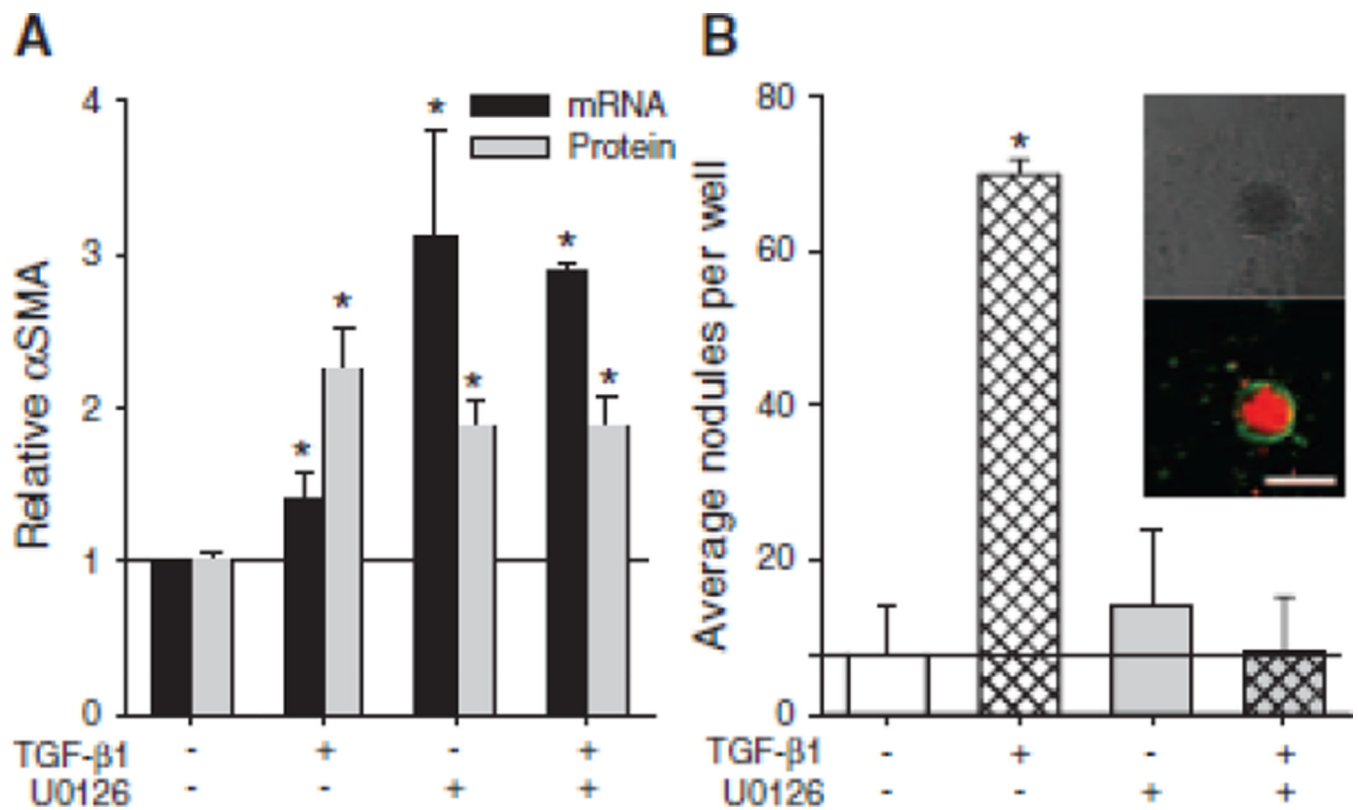
16. Benton JA, Kern HB, Leinwand LA, Mariner PD, Anseth KS. Statins block calcific nodule formation of valvular interstitial cells by inhibiting alpha-smooth muscle actin expression. *Arterioscler Thromb Vasc Biol.* 2009; 29:1950–1957. [PubMed: 19679827]
17. Fisher CI, Chen J, Merryman WD. Calcific nodule morphogenesis by heart valve interstitial cells is strain dependent. *Biomech Model Mechanobiol.* 2012
18. Jian B, Narula N, Li QY, Mohler ER 3rd, Levy RJ. Progression of aortic valve stenosis: Tgf-beta1 is present in calcified aortic valve cusps and promotes aortic valve interstitial cell calcification via apoptosis. *Ann Thorac Surg.* 2003; 75:457–465. discussion 465–456. [PubMed: 12607654]
19. Yip CY, Chen JH, Zhao R, Simmons CA. Calcification by valve interstitial cells is regulated by the stiffness of the extracellular matrix. *Arterioscler Thromb Vasc Biol.* 2009; 29:936–942. [PubMed: 19304575]
20. Chen JH, Yip CY, Sone ED, Simmons CA. Identification and characterization of aortic valve mesenchymal progenitor cells with robust osteogenic calcification potential. *Am J Pathol.* 2009; 174:1109–1119. [PubMed: 19218344]
21. Mohler ER 3rd, Gannon F, Reynolds C, Zimmerman R, Keane MG, Kaplan FS. Bone formation and inflammation in cardiac valves. *Circulation.* 2001; 103:1522–1528. [PubMed: 11257079]
22. Benton JA, Kern HB, Anseth KS. Substrate properties influence calcification in valvular interstitial cell culture. *J Heart Valve Dis.* 2008; 17:689–699. [PubMed: 19137803]
23. Cushing MC, Mariner PD, Liao JT, Sims EA, Anseth KS. Fibroblast growth factor represses smad-mediated myofibroblast activation in aortic valvular interstitial cells. *FASEB J.* 2008; 22:1769–1777. [PubMed: 18218921]
24. Gu X, Masters KS. Role of the mapk/erk pathway in valvular interstitial cell calcification. *Am J Physiol Heart Circ Physiol.* 2009; 296:H1748–H1757. [PubMed: 19363136]
25. Hinz B, Pittet P, Smith-Clerc J, Chaponnier C, Meister JJ. Myofibroblast development is characterized by specific cell-cell adherens junctions. *Mol Biol Cell.* 2004; 15:4310–4320. [PubMed: 15240821]
26. Lee DM, Kiener HP, Agarwal SK, Noss EH, Watts GF, Chisaka O, Takeichi M, Brenner MB. Cadherin-11 in synovial lining formation and pathology in arthritis. *Science.* 2007; 315:1006–1010. [PubMed: 17255475]
27. Schneider DJ, Wu M, Le TT, Cho SH, Brenner MB, Blackburn MR, Agarwal SK. Cadherin-11 contributes to pulmonary fibrosis: Potential role in tgf-beta production and epithelial to mesenchymal transition. *FASEB J.* 2012; 26:503–512. [PubMed: 21990376]
28. Merryman WD, Liao J, Parekh A, Candiello JE, Lin H, Sacks MS. Differences in tissue-remodeling potential of aortic and pulmonary heart valve interstitial cells. *Tissue Eng.* 2007; 13:2281–2289. [PubMed: 17596117]
29. Heupel WM, Baumgartner W, Laymann B, Drenckhahn D, Golenhofen N. Different ca2+ affinities and functional implications of the two synaptic adhesion molecules cadherin-11 and n-cadherin. *Mol Cell Neurosci.* 2008; 37:548–558. [PubMed: 18201900]
30. Hutcheson JD, Ryzhova LM, Setola V, Merryman WD. 5-ht(2b) antagonism arrests non-canonical tgf-beta1-induced valvular myofibroblast differentiation. *J Mol Cell Cardiol.* 2012; 53:707–714. [PubMed: 22940605]
31. Butcher JT, Tressell S, Johnson T, Turner D, Sorescu G, Jo H, Nerem RM. Transcriptional profiles of valvular and vascular endothelial cells reveal phenotypic differences: Influence of shear stress. *Arterioscler Thromb Vasc Biol.* 2006; 26:69–77. [PubMed: 16293796]
32. Pittet P, Lee K, Kulik AJ, Meister JJ, Hinz B. Fibrogenic fibroblasts increase intercellular adhesion strength by reinforcing individual ob-cadherin bonds. *J Cell Sci.* 2008; 121:877–886. [PubMed: 18303045]
33. Samarakoon R, Higgins PJ. Integration of non-smad and smad signaling in tgf-beta1-induced plasminogen activator inhibitor type-1 gene expression in vascular smooth muscle cells. *Thromb Haemost.* 2008; 100:976–983. [PubMed: 19132220]
34. Li J, Zhao Z, Liu J, Huang N, Long D, Wang J, Li X, Liu Y. Mek/erk and p38 mapk regulate chondrogenesis of rat bone marrow mesenchymal stem cells through delicate interaction with tgf-beta1/smads pathway. *Cell Prolif.* 2010; 43:333–343. [PubMed: 20590658]

35. Jiang W, Zhang Y, Wu H, Zhang X, Gan H, Sun J, Chen Q, Guo M, Zhang Z. Role of cross-talk between the smad2 and mapk pathways in tgf-beta1-induced collagen iv expression in mesangial cells. *Int J Mol Med*. 2010; 26:571–576. [PubMed: 20818498]
36. Greenberg RS, Bernstein AM, Benezra M, Gelman IH, Taliana L, Masur SK. Fak-dependent regulation of myofibroblast differentiation. *FASEB J*. 2006; 20:1006–1008. [PubMed: 16585062]
37. Simmons CA, Nikolovski J, Thornton AJ, Matlis S, Mooney DJ. Mechanical stimulation and mitogen-activated protein kinase signaling independently regulate osteogenic differentiation and mineralization by calcifying vascular cells. *J Biomech*. 2004; 37:1531–1541. [PubMed: 15336928]
38. Grossman M, Barsoum A, Lang S, Kaden JJ, Kallenbach K, Borggreffe M, Akat KM. Osteoblast-like differentiation in aortic valve stenosis is accompanied by changes in n-cadherin and cadherin-11 expression. *European Heart Journal*. 2010; 31:964. (Abstract).

\$watermark-text

\$watermark-text

\$watermark-text

**Fig. 1.**

The effect of MEK1/2 inhibition on hallmarks of dystrophic calcification. AVICs were treated TGF- β 1, U0126, U0126 + TGF- β 1 and assayed for α SMA and calcific nodule formation. MEK1/2 inhibition causes α SMA expression (A) but suppresses dystrophic calcific formation (B) in AVICs, both in the presence and absence of TGF- β 1. Inset in B shows calcific nodules with bright field and fluorescence microscopy, demonstrating an apoptotic outer ring surround a necrotic core. Scalebar = 250 μ m. All error bars indicate standard error of the mean. * indicates significant difference ($p < 0.005$) versus control.

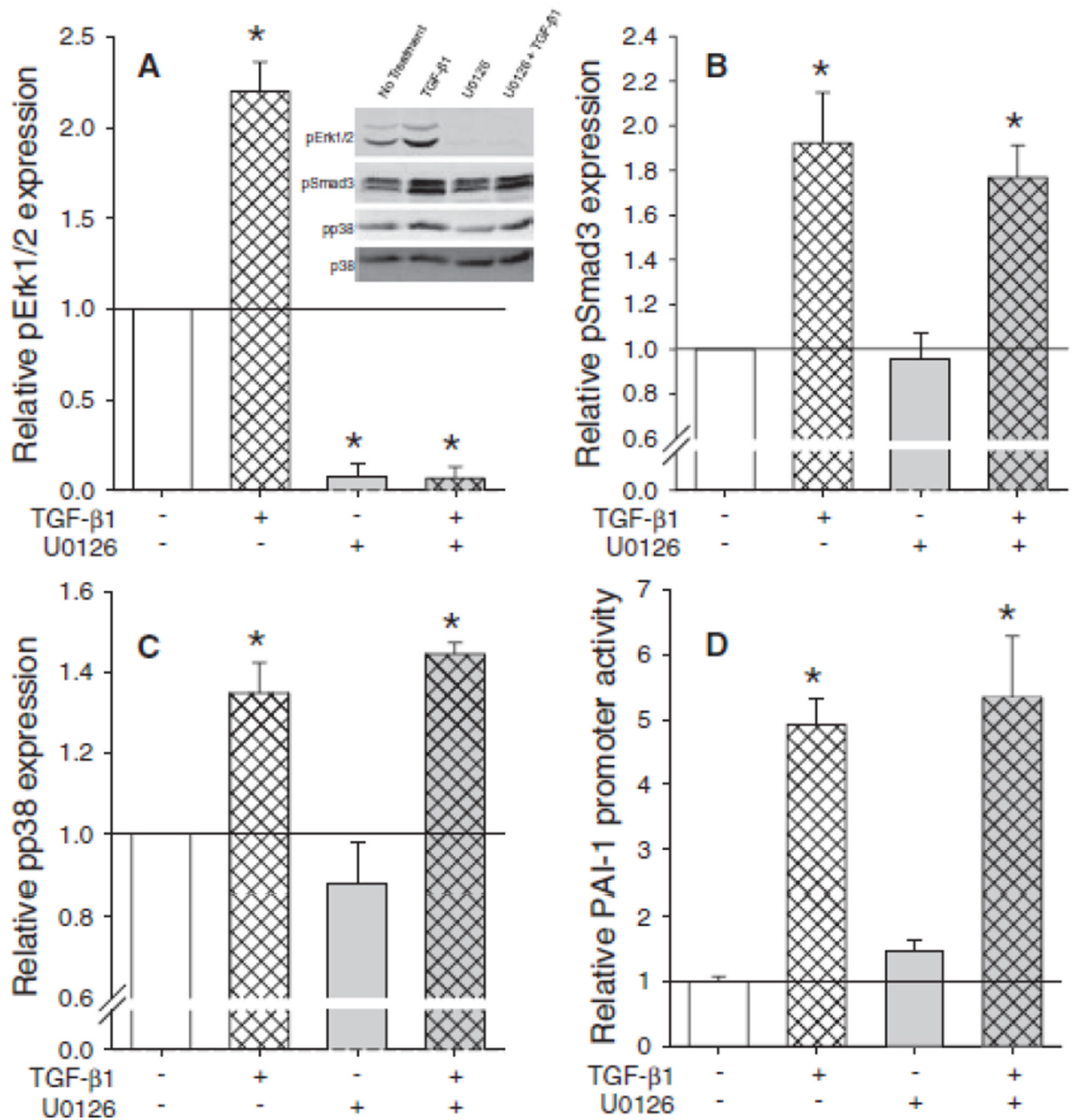


Fig. 2. U0126 does not interfere with canonical TGF- β 1 signaling. U0126 is a specific MEK1/2 inhibitor as indicated by the complete inhibition of pErk1/2 (A) but no change in pSmad3 (B) or pp38 (C). Inset in A shows representative blots and A-C are average densitometry from three independent experiments. Similar to the pSmad3 results, U0126 does not inhibit PAI-1 promoter activity following TGF- β 1 treatment (D). All error bars indicate standard error of the mean. * indicates significant difference ($p < 0.005$) versus control.

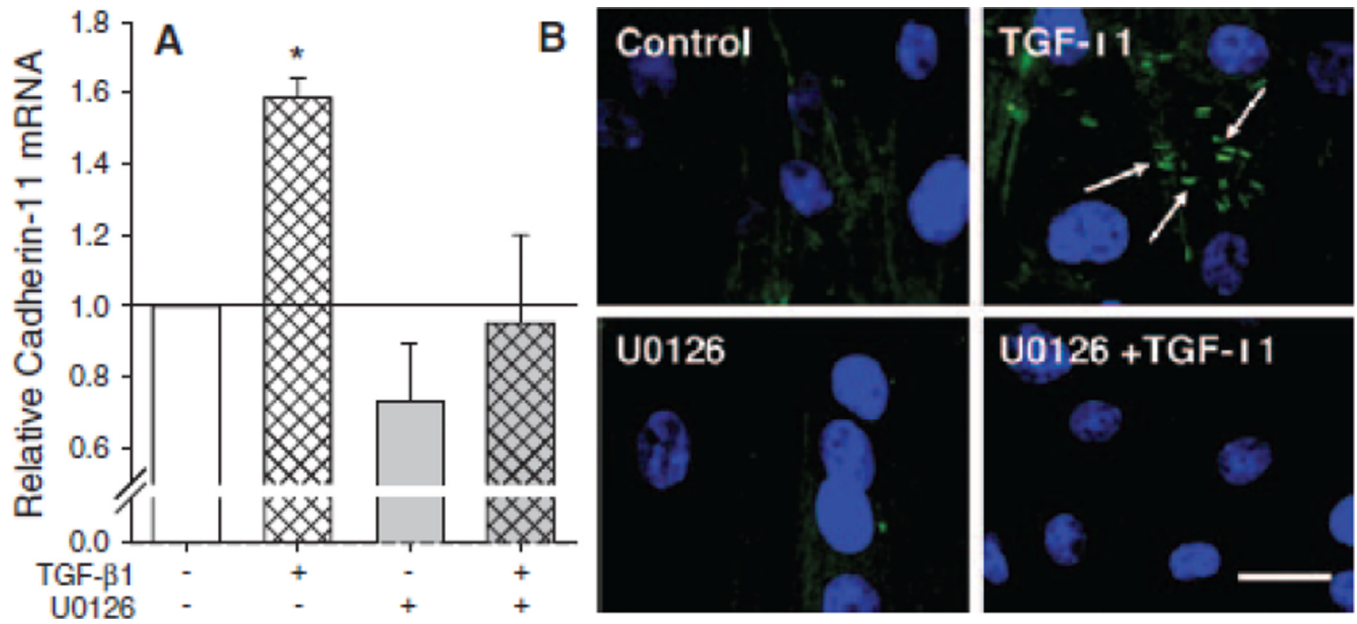
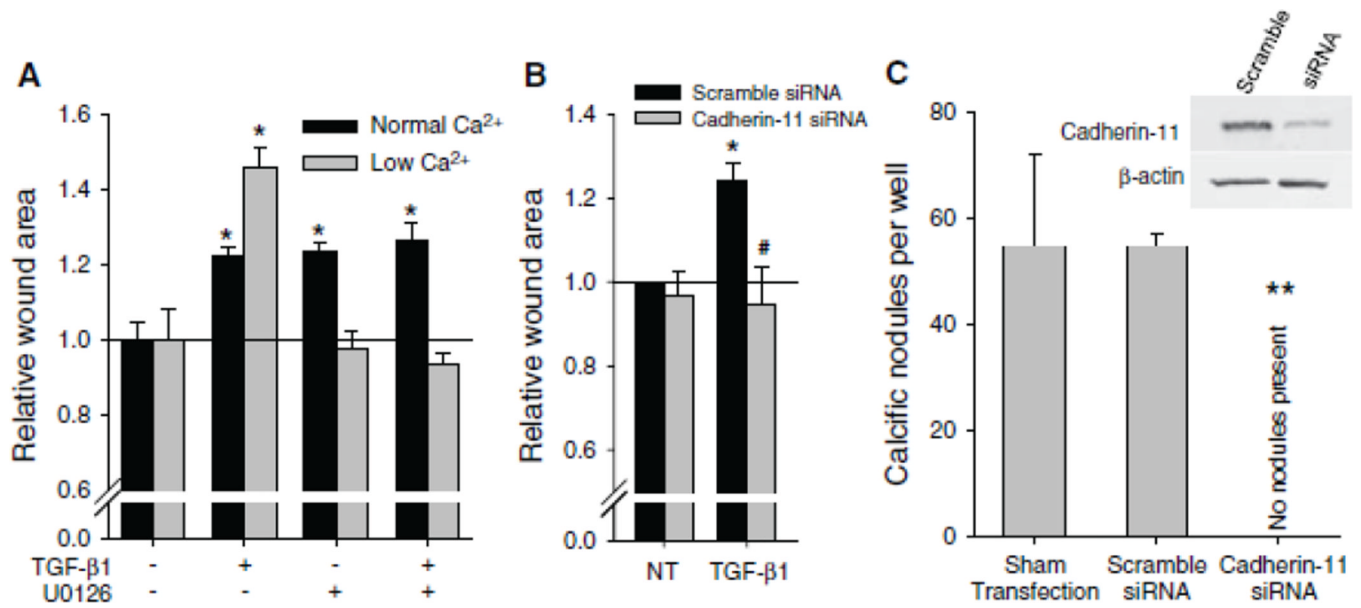


Fig. 3.

TGF-β1 incubation for 24 h increases cadherin-11 expression in AVICs. (A) pPCR reveals a 1.58 fold increase in cadherin-11 mRNA in samples treated with TGF-β1 and a decrease in cadherin-11 mRNA with inhibition of MEK1/2. (B) Immunostaining shows cadherin-11 in TGF-β1 groups with minimal to no stain in other treatment groups. Scalebar = 10 μm. All error bars indicate standard error of the mean. * indicates significant difference (p < 0.005) versus control.

**Fig. 4.**

Cadherin-11 generates intercellular tension through α SMA that enables calcific nodule morphogenesis. (A) Wound assay reveals strength of intercellular connection which correlates to wound area. At normal Ca^{2+} levels, with all cadherins functional, TGF- β 1, U0126, and U0126 + TGF- β 1 treatments all increased wound area size due to increased α SMA expression. However, at low Ca^{2+} levels, where cadherin-11 is still functional and others are not, TGF- β 1 treated cells created a large wound. (B) siRNA knockdown of cadherin-11 in physiologic Ca^{2+} media decreases TGF- β 1 initiated wound area to control levels. (C) siRNA knockdown of cadherin-11 prevents calcific nodules. Inset Western blots show that cadherin-11 is knocked down at the time of the wound assay and calcific nodule experiments. All error bars indicate standard error of the mean. * indicates significant difference ($p < 0.005$) versus control. # indicates significant difference ($p < 0.05$) versus Scramble. ** indicates significant difference ($p < 0.005$) versus Sham and Scramble.

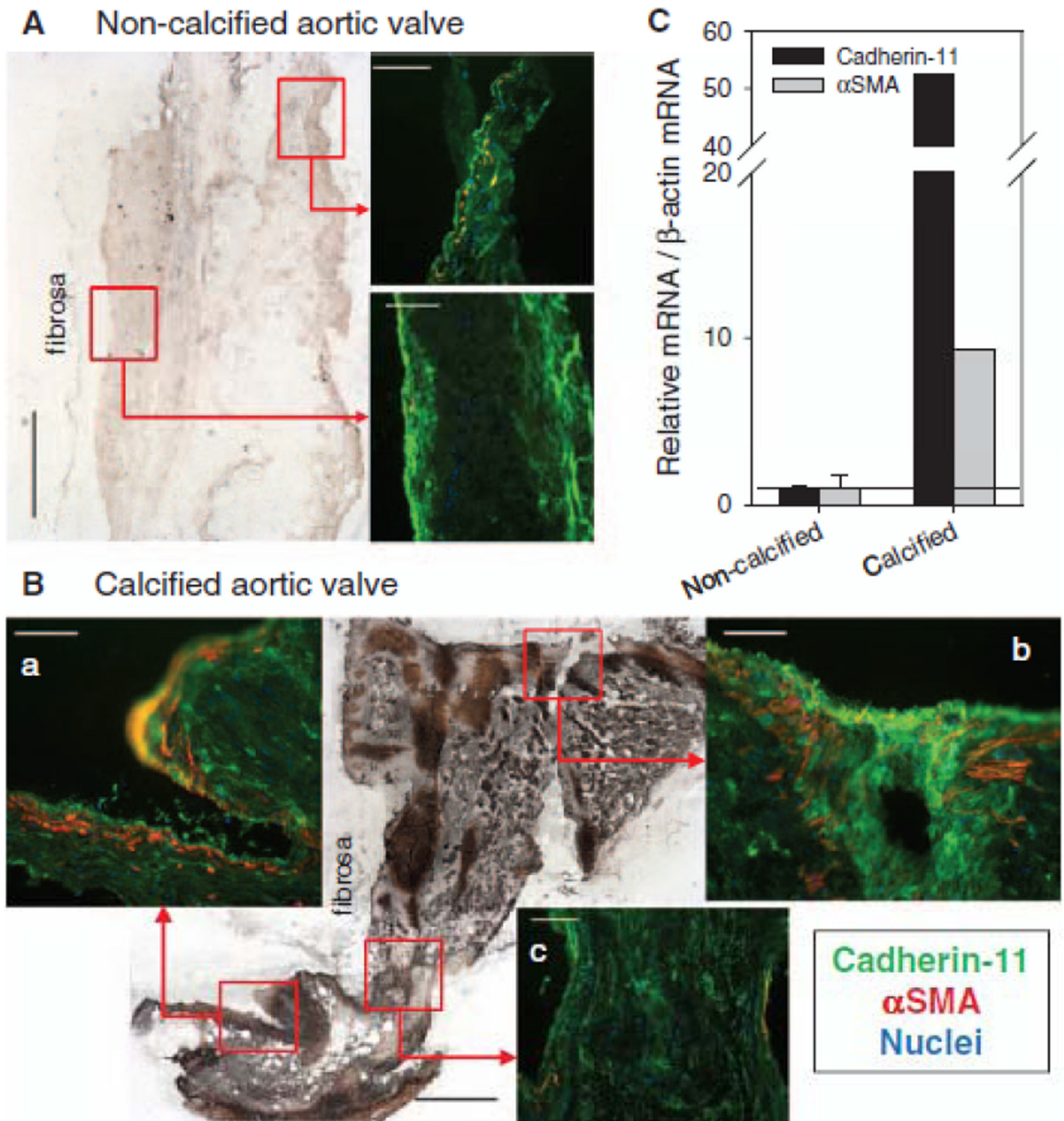


Fig. 5. Cadherin-11 and α SMA expression are increased in calcified human aortic valve leaflets. (A) Immunostaining of a non-calcified leaflet reveals cadherin-11 expression along the periphery of the leaflet, sparse α SMA staining, and very little calcification indicated by the von Kossa stain. (B) Calcified leaflet shows enriched cadherin-11 and α SMA co-localization in areas of significant calcification (panels a and b), as seen in the von Kossa stain, but not in areas where calcification is less intense (panel c). (C) mRNA for cadherin-11 and α SMA are increased in the calcified leaflet (n=1) compared to the non-calcified leaflets (n=2). Scalebar = 500 μ m for von Kossa; = 100 μ m for immunofluorescence.